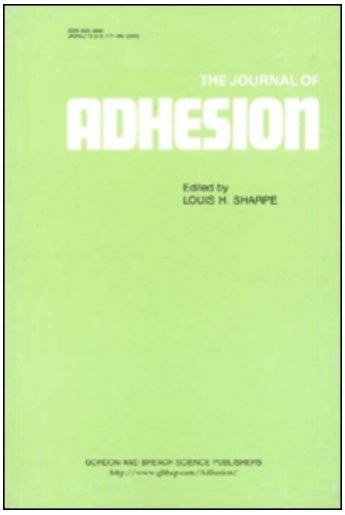

The Journal of Adhesion
Publication details, including instructions for authors and subscription information:
http://www.informaworld.com/smpp/title~content=t713453635

The Use of Large Diameter Monofilament for Improving Peel Resistance of a Brittle High Temperature Adhesive

S. Azam; J. P. Sargent[a]
[a] Sowerby Research Centre, British Aerospace, Bristol, UK

Online publication date: 02 December 2010

To cite this Article Azam, S. and Sargent, J. P.(1999) 'The Use of Large Diameter Monofilament for Improving Peel Resistance of a Brittle High Temperature Adhesive', The Journal of Adhesion, 71: 1, 1 — 20
To link to this Article: DOI: 10.1080/00218469908009563
URL: http://dx.doi.org/10.1080/00218469908009563

J. Adhesion, 1999, Vol. 71, pp. 1–20
Reprints available directly from the publisher
Photocopying permitted by license only

The Use of Large Diameter Monofilament for Improving Peel Resistance of a Brittle High Temperature Adhesive

S. AZAM[a] and J. P. SARGENT[b,*]

[a] *106 Shaggy Calf Lane, Slough, Berkshire, SLZ 5HQ, UK;*
[b] *British Aerospace, Sowerby Research Centre, FPC 267, P.O. Box 5, Filton, Bristol, BS34 7QW, UK*

(Received 19 January 1999; In final form 11 March 1999)

Peel force measurements as a function of adherend thickness are reported for adhesively bonded specimens based on a cyanate ester resin and aluminium adherends. It has been demonstrated that by incorporating large diameter (0.28 mm) PTFE monofilament within the adhesive bond then the peel force and associated fracture energy can be increased significantly over that for specimens based on adhesive alone. Fracture energy measurements are derived for specimens with peeling adherend thickness of up to about 0.6 mm using the 90° peel test. Fracture energies are also derived for peeling of more practically-representative 1.6 mm thickness adherends using a single cantilever beam experiment. *In-situ* photoelasticity and SEM microextensometry experiments are reported which show the stress fields and displacements associated with the presence of the monofilament. It is believed that the reported increase in measured fracture energy is partly due to the crack pinning effect of the monofilament, and partly due to the monofilament creating a "load shadowed" region between adherend and monofilament which prevents the interfacial crack from propagating between adherend and adhesive.

Keywords: High temperature adhesives; aluminium; peel testing; single cantilever and double cantilever beam testing; physical modifications; fracture energy; stress state

INTRODUCTION

Adhesives based on cyanate resin esters have the potential for offering an improvement over epoxy-based systems for long-term, high-temperature performance. Unfortunately, however, when compared

*Corresponding author.

with modern toughened epoxy resins these systems are very brittle. For the aerospace industry, this brittleness would normally translate into unacceptably low values of fracture toughness as manifest in, for example, the peel or double cantilever beam test. The primary aim of the work described here is to improve fracture strength as measured using the peel test by introducing a discrete second phase into the adhesive. This builds on experience gained previously, where it was found that the presence of relatively large diameter nylon monofilament in a carrier-based epoxy adhesive modified the stress field within the adhesive and increased the peel strength [1]. Although the exact toughening mechanism was not identified, it was found that debonding of the monofilament created a "load shadowed" region between monofilament and the adherend with reduced load. This reduced load region in turn prevented cracking from proceeding along the adhesive/adherend interface and, because of the stress concentration created by the monofilament, precipitated cohesive failure within the adhesive. This basic idea of incorporating large diameter monofilament has been exploited here by using PTFE monofilament in order to achieve a similar crack deflection and toughening action. *In-situ* peeling experiments are also described which use microextensometry within the SEM and photoelasticity with an optical microscope, permitting mapping of the displacement and stress fields within the adhesive bond.

SPECIMENS AND EXPERIMENTAL DETAILS

Specimen Preparation

All adhesive specimens were made using a cyanate ester resin, AroCy-B10 or AroCy-M10, with clad and non-clad aluminium alloy 2024T3 adherends. The adherend surfaces were all pretreated by degreasing and chromic sulphuric acid etching. Those specimens in which monofilament was also included were made by first carefully winding a continuous 0.28 mm PTFE monofilament repeatedly across the width of an adherend surface, and then adding adhesive. This gave a specimen with a uniform array of parallel monofilament present in the bond line with a pitch of 0.7 mm. All specimens were usually 25.4 mm

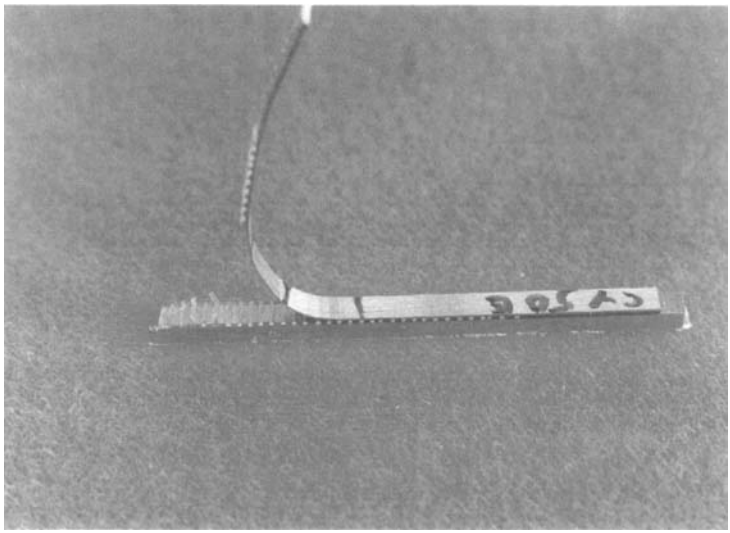

FIGURE 1 Photograph of the small 2 mm wide peel specimen. (See Color Plate I).

wide, with overlaps up to approximately 75 mm, and adherend thickness of 1.6 mm. These were then subsequently cut to 2 mm widths to give specimens suitable for either peel, double cantilever beam (dcb) or single cantilever beam (scb) testing. Peel specimens were then further prepared to give a range of peeling adherend thickness by carefully polishing one of the adherends to give an adherend of constant thickness, usually in the range between about 50 μm and 600 μm. Figure 1 shows an example of a small 2 mm wide peel specimen. Curing for the B10 resin was 2 hours at 200°C and for the M10 resin was 20 hours at 180°C and 2 hours at 240°C.

Specimen Testing

Three different geometries were selected for measurements of fracture energies. These were the 90° peel test, the double cantilever beam test and the single cantilever beam test. One of the aims of the work described here was to demonstrate improved peel performance for specimens with thickness up to the nominal "industry standard" adherend thickness of 0.6 mm as used in the floating-roller peel test.

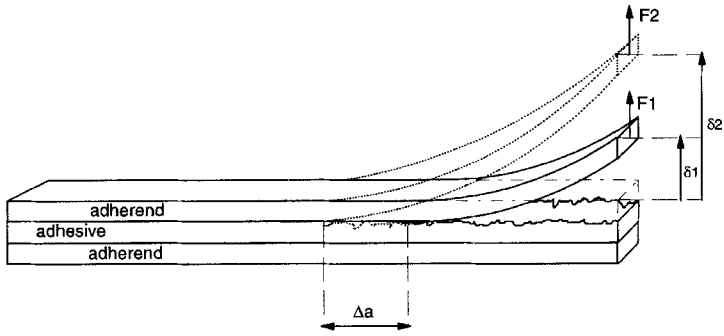

FIGURE 2 Schematic diagram showing the geometry of the scb test and nomenclature used in the analysis. The top adherend forms the single cantilever beam and the lower adherend is firmly gripped in the jaws of the testing machine.

However, because practical aerospace structures would not normally use such thin adherends, it was also relevant to extend peeling results to 1.6 mm thick adherends. Peel testing with such thick adherends is not very practical because of the large peeling adherend radii of curvature required, necessitating very long specimens. An alternative test that gives a similar stress distribution at the peel front is the single cantilever beam test. So long as adherend yielding does not occur, fracture energies can be measured without the need for very long specimens. The scb test is shown schematically in Figure 2. Note that the top adherend formed the single cantilevered beam, whilst the lower adherend was rigidly secured in the grips of the testing machine. Double cantilever beam specimens were also included; these served as a reference for measurement of fracture energies when failure was purely cohesive within the adhesive. Peel testing was performed using a peeling rate of 1 mm/minute, and scb and dcb testing was undertaken with a crosshead speed of between 0.2 mm/minute and 0.5 mm/minute.

Microextensometry and Photoelasticity Specimens

Microextensometry peel specimens were made which were suitable for *in-situ* observation of surface displacements within the SEM. These were prepared from the larger 2 mm wide specimens above using a procedure given in Ref. [1] which entailed deposition of gold through a TEM grid in order to obtain a grid pattern on the polished edge of

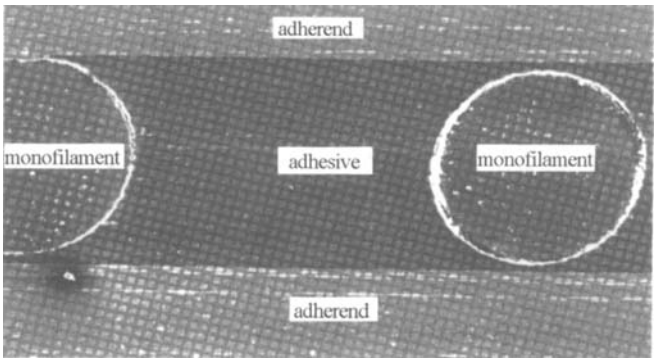

FIGURE 3 SEM image of the edge of a small peel specimen showing the disposition of adherend, adhesive and PTFE monofilament. A grid pattern of small squares with pitch of 12.5 μm has been deposited on the surface.

a small peel specimen. Specimens were approximately 0.5 mm wide, with a peeling adherend thickness of 0.3 mm. The grid was composed of a repeating pattern of small squares with a pitch of 12.5 μm, and by taking images before and during the peeling process, it was possible to map surface displacement in the adhesive bond line in detail. Figure 3 shows an example of the resulting grid pattern.

Photoelasticity peel specimens were also made in the same fashion as described above, but instead of depositing a grid pattern on the specimens the sides were optically polished in order to render them transparent. A small purpose-designed straining rig was designed and built for *in-situ* straining on an optical microscope stage, and observations were made of the photoelastic patterns which developed within the adhesive bond line during peeling. A photograph of the straining rig is shown in Figure 4.

THEORY

The extraction of fracture energies using the peel test was performed by conducting a best fit to the experimental data using the analysis of Moidu *et al.* [3]. Briefly, this analysis used an energy release rate which was considered to reflect the energy to break the interfacial bonding forces and the energy dissipated locally ahead of the peel front in the

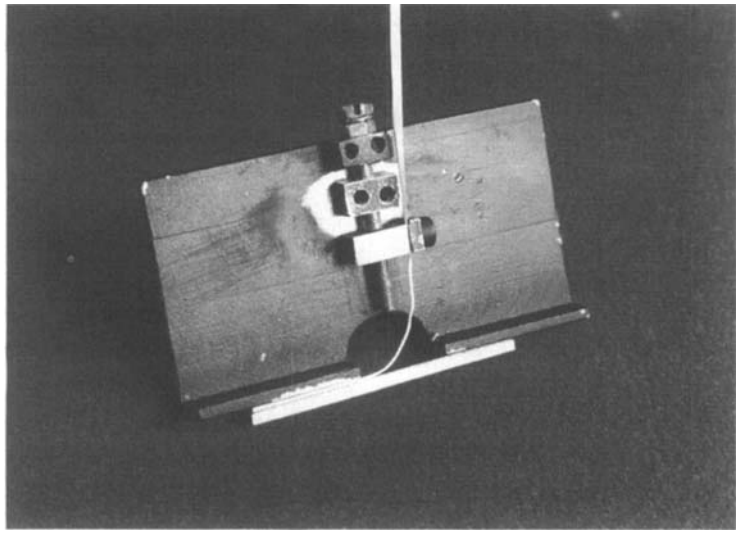

FIGURE 4 Photograph showing the small straining rig designed for *in-situ* testing of specimens on the stage of an optical microscope. A peel specimen is shown mounted in the rig. The stage measures approximately 4 cm × 7 cm. (See Color Plate II).

plastic or viscoelastic zone. In order to do this, the analysis also had to consider the stored strain energy within the peeling arm, the energy dissipated during tensile deformation of the peeling arm, and the energy dissipated due to bending of the peeling arm. The solutions, which are too lengthy to be included here, are in the form of a set of simultaneous equations which can be solved numerically using an iterative technique. In practice, for a given fracture energy, this generally resulted in plots of peel force which depended sensitively on adherend yield strength and adherend thickness.

Double cantilever beam fracture energy was extracted using theory given by Fernlund and Spelt [5] which explicitly account for the thickness and material properties of an adhesive layer using a beam on an elastic foundation model:

$$G_I^A = \frac{12(Fa)^2}{Eh^3b^2(1-t/h)^3}\left[1+0.639\left\{(1-t/h)^3[1+t/h(2E/E_a-1]\right\}^{0.25}h/a\right]^2$$

where: G_I^A = Mode I fracture energy
F = Load applied to the specimen
a = crack length
E = Young's modulus of the adherends
E_a = Young's modulus of the adhesive layer
h = beam arm height
t = half thickness of the adhesive layer
b = specimen width

Extraction of fracture energies using the single cantilever beam test was obtained by using a simple approach which required measurements of the crack propagation distances and measurement of the equivalent areas under the load/displacement graph [4].

For elastic behaviour the fracture energy is given by:

$$G_I^A = \Delta U / b \Delta a$$

where: ΔU = energy required to propagate crack over a length Δa.

Then, with reference to the schematic diagram shown in Figure 2, if the load and displacement are linear, it is easily shown that ΔU_1 can be approximately calculated using $\Delta U_1 = 0.5(F_1\delta_2 - F_2\delta_1)$, where the subscripts 1 and 2 refer to loads (F) and displacements (δ) at the beginning and end of an increment in crack growth defined by the area ΔU_1.

Note that extraction of fracture energies using the peel test and dcb test was based on adherends with Young's modulus of 71.4 GPa (E) and, unless otherwise stated, a yield strength of 310 MPa (σ_y), with an adhesive with Young's modulus of 1.8 GPa (E_a). The adhesive half-layer thickness (t) was approximately 0.14 mm for the PTFE monofilament-based specimens, and approximately 0.125 mm for the specimens without monofilament.

RESULTS

Peel forces as a function of adherend thickness up to about 150 μm are shown in Figure 5 for specimens based on M10 adhesive with clad adherends, and on B10 adhesive with non-clad adherends. High

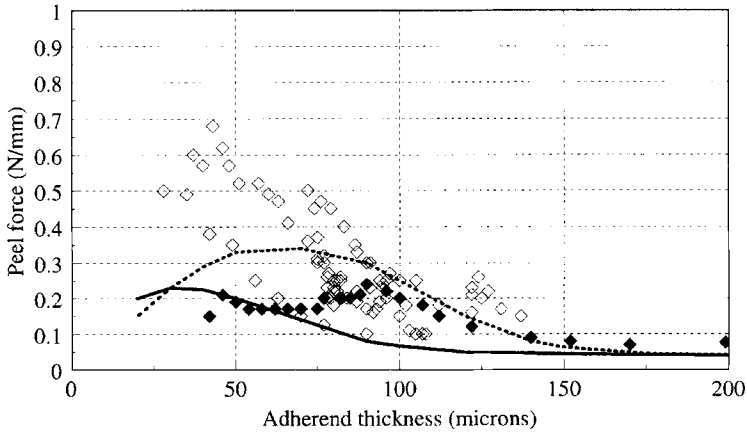

FIGURE 5 Peel force as a function of adherend thickness for cyanate adhesives based on B10 resin and non-clad adherends (◆), and M10 resin and clad adherends (◇). The lines are based on predictions using fracture energies of 40 J/m^2 for clad (dashed line) and non-clad (solid line) aluminium.

resolution SEM images of the peeled adherend and adhesive surfaces for the M10 specimens with clad adherends are shown in Figure 6. SEM images are also shown in Figure 7 for the B10 specimens with non-clad adherends. Note that the SEM images showed that the adhesive surface after peeling in both cases formed reasonable replicas of the adherend surfaces, with the detailed pore structure clearly visible, indicating that failure occurred at the interface between adherend and adhesive. Careful inspection of the adhesive surface shown in Figure 7b does, however, show that there is a population of small "fingers" sticking up from the adhesive surface which do not appear to have a uniform distribution, but are instead rather fragmented. Careful inspection of the opposite adherend surface also shows that some of the pores are apparently not present. This suggests that some of the fingers on the adhesive surface have broken off and, in some regions, now fill in the pores. It is not clear, however, whether the fingers are oxide, adhesive, or both.

Figure 5 also shows the theoretical peel forces derived using the analysis of Moidu *et al.* [3] for a fracture energy of 40 J/m^2. Note that two curves are shown; one is based on 2024T3 aluminium adherends with uniform yield strength of 310 MPa across the adherend thickness,

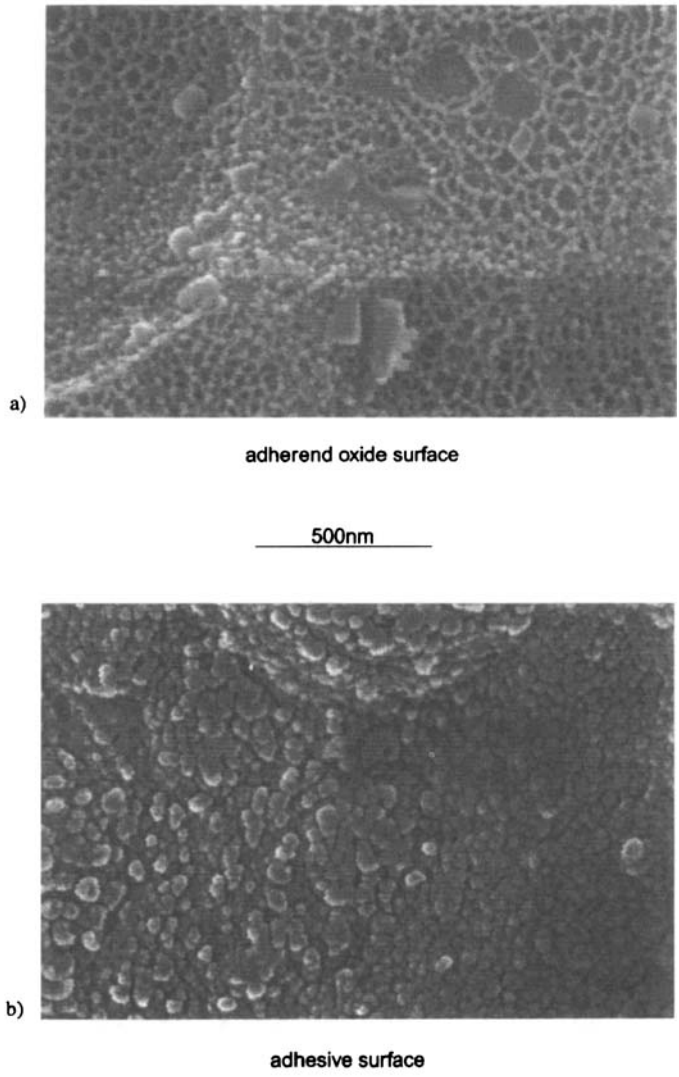

FIGURE 6 High resolution SEM images of the adherend (a) and adhesive (b) fracture surfaces after peeling for M10 adhesive and clad adherends.

and the other is shown where the adherend has been modelled to take account of the presence of a cladding layer present on the adherend surface. Cladding layer thickness was measured at 50 μm using a micro-hardness apparatus, and a yield strength of the cladding layer of

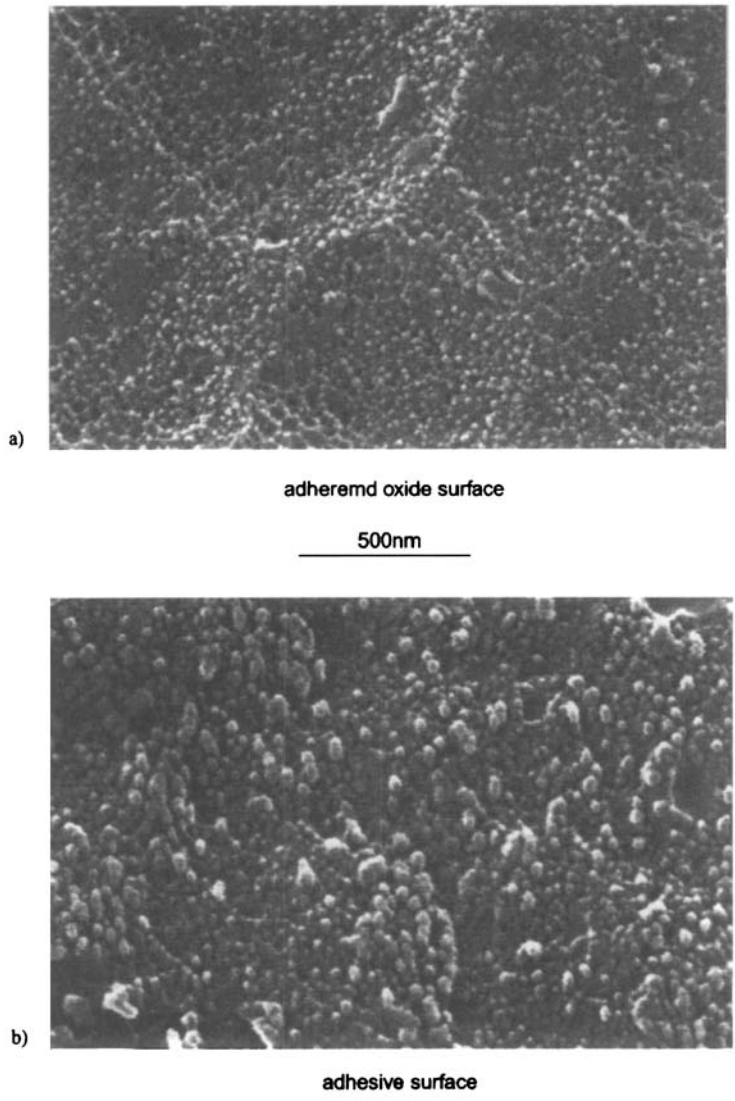

FIGURE 7 High resolution SEM images of the adherend (a) and adhesive (b) fracture surfaces after peeling for B10 adhesive and non-clad adherends.

50 MPa was assumed for the analysis. Corrections to the predictions were undertaken by assuming that the net adherend yield strength could be modelled by assuming an average yield strength which

depended on the fractional thickness of a pure aluminium clad layer and 2024T3 alloy. Note that this procedure, whilst not completely satisfactory, does improve the fit to the experimental data. It should also be noted that the above modelling has taken no account for changes in mode I/mode II ratios as a function of adherend thickness. It is possible that by including this within the analysis that further improvement between experiment and theory could have been obtained.

Peel force as a function of adherend thickness up to about 0.6 mm is shown in Figure 8 for specimens comprising clad adherends with B10 adhesive and PTFE monofilament. SEM images of the peeled adherend and adhesive surfaces are shown in Figure 9. Note that comparison of Figure 8 with Figure 5 shows that peel force was significantly increased. Inspection of Figure 9 shows that cracking is no longer interfacial as observed earlier in Figures 6 or 7, but is instead cohesive, with the crack repeatedly arrested and then precipitated within the adhesive at successive monofilament locations. Figure 8 also shows the results of a best fit to the data using the above analysis and a fracture energy of 300 Jm^2.

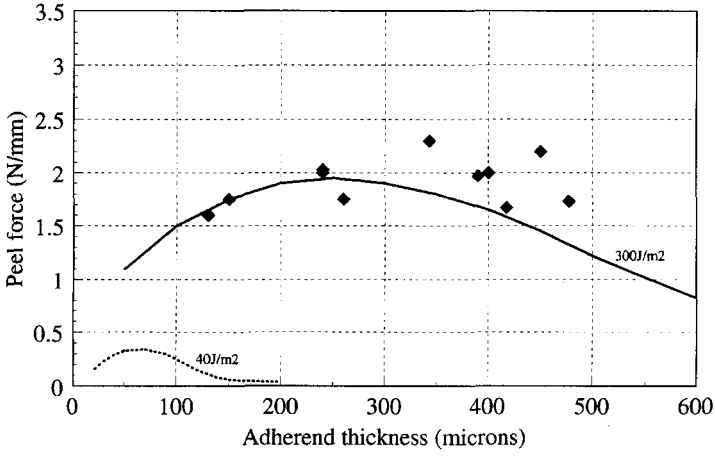

FIGURE 8 Peel force as a function of adherend thickness for cyanate adhesive based on B10 resin with 0.28 mm PTFE monofilament and clad adherends (◆). The lines are based on predictions using fracture energies of 40 J/m^2 (dashed line) and 300 J/m^2 (solid line).

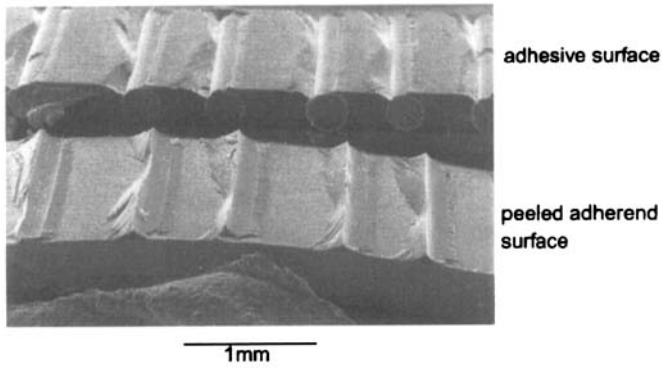

FIGURE 9 SEM images of the adherend and adhesive fracture surfaces after peeling for B10 adhesive comprising PTFE monofilament and clad adherends. Peeled adherend approximately 0.4 mm thick. Note the cracking with respect to monofilament position.

The single cantilever beam experiment gives a similar peeling action as observed above, but permits fracture energy measurements with much thicker adherends. Scb results on B10 specimens with PTFE monofilament using clad 1.6 mm adherends gave a fracture energy of $350 \pm 90\,J/m^2$ (average $\pm$ standard deviation). Dcb measurement on a B10 specimen with PTFE monofilament and 1.6 mm clad adherends gave a fracture energy of $335 \pm 58\,J/m^2$. SEM images for both the scb and dcb fracture surfaces are shown in Figures 10a and 10b, respectively. Note that in the above SEM images, the peeling action biases fracture towards the peeling adherend, whilst in the dcb test, fracture is biased towards the centre line of the bond. Scb and dcb measurements on specimens with 1.6 mm thick adherends, similar to that used above, but without additional monofilament, gave values of $60 \pm 12\,J/m^2$ and $230 \pm 75\,J/m^2$, respectively. Failure surface examination for these specimens without additional monofilament showed adhesive failure for the scb specimens, indistinguishable in appearance from that seen for the earlier peel specimens shown in Figures 6 or 7 above. The failure surface for the dcb specimen showed cohesive failure. Table I summarises the fracture energy values recorded for each of the peel, scb and dcb specimens both with and without additional monofilament.

Figure 11 shows photoelasticity patterns observed with linear polarised light for a small B10 peel specimen with PTFE monofilament

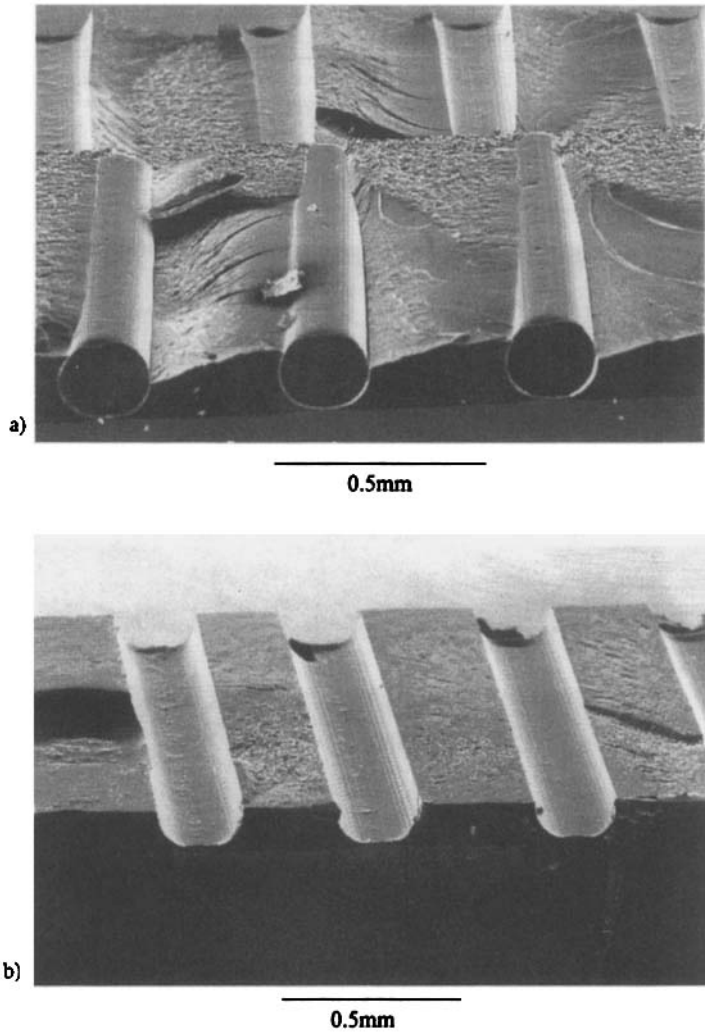

FIGURE 10 SEM images of the adherend and adhesive surfaces for specimens comprising 1.6 mm clad adherends with B10 adhesive and PTFE monofilament: (a) peeled adherend and adhesive fracture surfaces using the single cantilever beam experiment; (b) peeled adhesive fracture surface using the double cantilever experiment.

with peeling adherend of 0.4 mm thickness, (a) with no load, (b) during peeling just prior to crack propagation and, (c) just after fracture has occurred and using monochromatic light for illumination. In the no-load image (a), the polarisation direction is parallel to the plane of the

TABLE I Summary of measured fracture energies for specimens with and without PTFE monofilament. Scb and dcb quoted values are averages with standard deviations

Specimen	*Fracture energy from peel expt.* (J/m^2)	*Fracture energy from scb expt.* (J/m^2)	*Fracture energy from dcb expt.* (J/m^2)
No monofilament	~ 40	60 ± 12	230 ± 75
With monofilament	~ 300	350 ± 90	335 ± 58

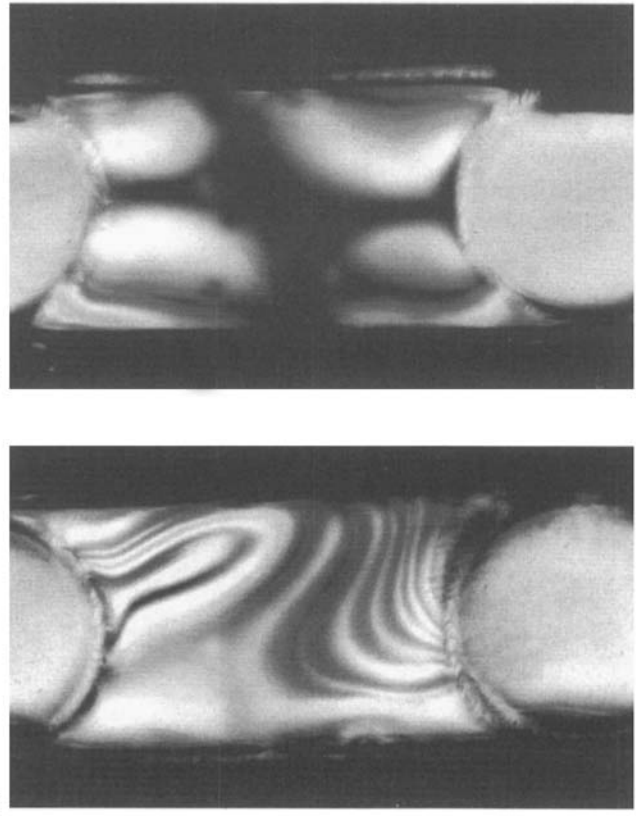

FIGURE 11 Photoelastic fringes taken during an *in-situ* peel of a small adhesive specimen comprising PTFE monofilament and cyanate B10 adhesive. Image (a) shows the specimen with no load indicating the residual stress pattern, and (b) under load with the top adherend peeling and the crack pinned at the right monofilament, and (c) in monochromatic light after the crack has run between monofilaments. (See Color Plate III).

bond, and shows a combination of isoclinics (the black cross-shaped feature between the monofilaments) and isochromatics (the coloured fringes towards the top and bottom of the bond line). The isoclinics

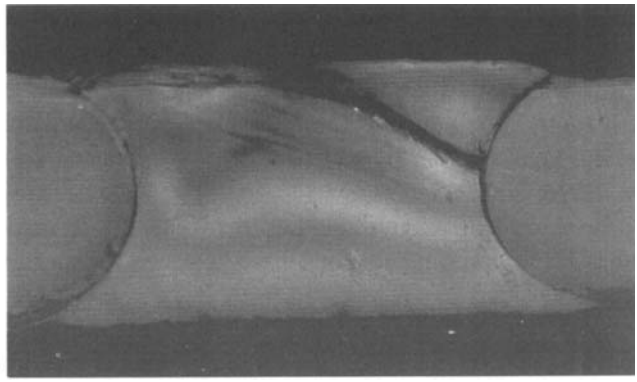

FIGURE 11 (Continued).

show that at every point along the line where the black line exists, the principal stresses run parallel and perpendicular to the bond line. The isochromatics, indicating principal stress differences, arise from the residual stress pattern between monofilament locations, probably as a result of cure shrinkage and thermal expansion effects originating during cooling from the cure temperature. In the loaded image (b), the polarisation direction is at 45° to the plane of the bond line. In this instance, the peeling adherend is at the top of the image and the crack front has been arrested by the monofilament at the right of the image, with the resulting stress field generating the complicated birefringence pattern between the monofilament locations. Inspection of image (c) after failure has occurred shows the fracture path between monofilaments and the birefringence patterns after loading. Comparison with the earlier images shows that the complicated birefringence pattern that existed under load no longer exists, indicating that little or no plastic deformation occurred in the bulk of the adhesive during deformation and fracture. This would suggest that load which was sustained during peeling was by stored elastic energy throughout a significant proportion of the bond line thickness, which was then released and dissipated during fracture.

Figure 12 shows grid patterns of the surface displacement for a B10 specimen with clad adherends with a peeling adherend thickness of approximately 300 μm, (a) with no load and in (b) under load and just before crack propagation. The peeling geometry is the same as used in the above photoelasticity images, *i.e.*, with the peeling adherend at the top of the image with the crack arrested at the right hand monofilament.

Inspection of the region between the right-hand monofilament and adherend in image (b) shows debonding between monofilament and adhesive. This arrested the main peeling crack that would otherwise have propagated along the interface between adherend and adhesive. A composite image showing the net surface displacement that occurred between images is shown in Figure 12c. In this image, lines are drawn to indicate displacement magnitudes and arrows indicate displacement directions. It is interesting to note, from a general inspection of the

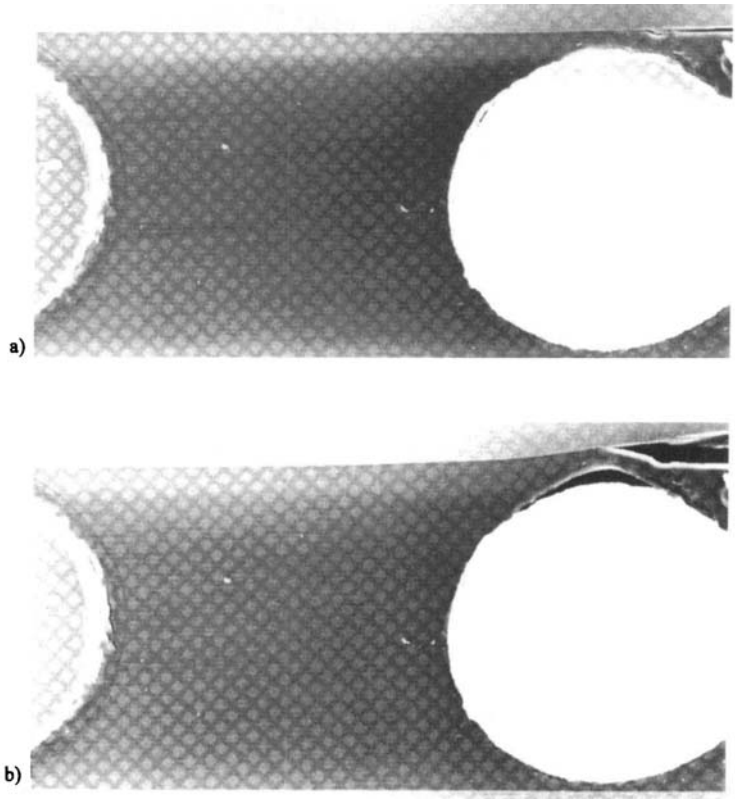

FIGURE 12 Grid patterns and surface displacement recorded during an *in-situ* SEM peel of a small specimen comprising PTFE monofilament and cyanate B10 adhesive. Image (a) shows the specimen with no load, and (b) under load with the top adherend peeling and the crack pinned at the right monofilament, and in (c) the net surface displacement between images (a) and (b). The small lines show the magnitude of the surface displacements, and the arrows indicate the directions.

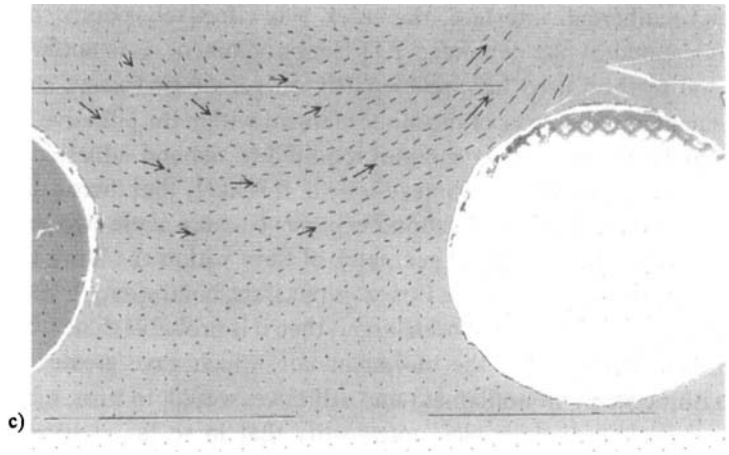

FIGURE 12 (Continued).

displacements and directions, that the peeling action not only results in a tensile strain region normal to the bond line adjacent to the right-hand monofilament, but also a compressive strain region normal to the bond line approximately to the left of centre of the image. Note that this compressive region has been both predicted and observed experimentally in other work on the peel test, see, for example, Kaeble and Ho [6], Kim and Aravas [7].

DISCUSSION

The incorporation of large-diameter PTFE monofilament into the bond line of specimens made with a cyanate adhesive has successfully increased peel forces from ~ 0.3 N/mm and fracture energies of ~ 40 J/m^2 to peel forces ~ 2 N/mm and fracture energies of ~ 300 J/m^2. This technique relied upon the poor adhesion between PTFE and the adhesive, which reduced load transfer to the region between monofilament and adherend. This, in turn, gave an interfacial region which was sufficiently unstressed to prevent the interfacial crack from propagating further along the interface between adhesive and adherend. In consequence, the crack was forced to propagate within the adhesive. Note that once the crack locus had been shifted away from the

adhesive/adherend interface, the crack was effectively pinned by the cavity created by the debonded PTFE monofilament. It is noteworthy that the method used here relies partly on geometric factors such as placement and diameter of the monofilament within the adhesive bond, and partly on the relative energies required to debond adhesive from monofilament or adhesive from adherend. It is likely that there exists an optimum balance between debond energies between these two regions and between placement and geometry of fibre within the bond line in order to maximise peel forces. For example, if the bond strength between adherend and adhesive had been larger, then it is probable that choice of a different material for the monofilament, which gave greater bond strength between monofilament and adhesive, would, in turn, have increased peel force. It is also noteworthy that in so far as geometric factors are involved which alter the local stress field (and precipitate cohesive failure), then the method described here is applicable as a general strategy for improving peel resistance in all adhesives which would otherwise fail at the interface between adhesive and adherend.

In a previous paper [1], it was demonstrated that peeling adherend thickness plays an important part in determining the uniformity of the stress field throughout the adhesive bond line. This, in turn, influences the interaction with inclusions (such as monofilament, carrier cloth, *etc.*) within the adhesive, and the final measured peel forces and fracture energies. As a general rule, therefore, care should be exercised when undertaking the peel test that a judicious choice of adherend thickness is made in order to ensure that derived fracture energies and peel forces are actually from tests which are representative of failure conditions likely to be encountered in practice. In reality, this might mean, for example, that fracture energies derived using a scb test with 1.6 mm adherends could be more valid than fracture energies derived with a peel test using 0.6 mm adherends.

The use of hand winding of monofilament is clearly not a practical method for improving peel performance; however, it does serve to illustrate the underlying mechanisms which can be exploited for increasing peel strength. Incorporation of knitted and woven monofilament is a more practical method for specimen manufacture, and is indeed used for manufacture with modern adhesive as a means of adhesive support and for control of bond line thickness. It should also be noted, however, that the stress field that arises as a result of the

interaction between monofilament and peeling adherend when using a woven or knitted monofilament is likely to depend also on the degree of consolidation between resin and fibre, the bond line thickness, the testing direction with respect to any preferred orientation (such as a weave direction), and also the interfacial bond strength between monofilament and resin.

CONCLUSIONS

The incorporation of large-diameter PTFE monofilament has successfully increased the fracture toughness of a cyanate ester resin adhesive, as measured using peeling tests, from $\sim 40\,J/m^2$ to over $300\,J/m^2$. This has been demonstrated by measurements using a conventional peeling arrangement with specimens comprising adherends up to 0.6 mm thickness, and with single cantilever beam specimens comprising adherends with 1.6 mm thickness. It should be emphasised that this increase in measured fracture energy is due to the shifting of the failure location away from the interface between adherend and adhesive, and into the adhesive. Since it is a physical method, which relies on modification of the stress field within the adhesive, it is applicable as a general method for improving peel strength for all adhesives where premature interfacial failure occurs between adherend and adhesive.

Acknowledgements

The authors would like to thank Dr. C. Uhlig and Prof. M. Bauer of the Aussenstelle Polymermaterialien und Composite of the Fraunhofer Institut Zuverlassigkeit und Microintegration for the supply of the pre-polymerised resin. They would also like to thank Dr. D.G. Dixon for his help during the project. This work was carried out under the auspices of a BRITE-EURAM III project, No: BRPR-CT97-0418.

References

[1] Sargent, J. P., "Microextensometry, the peel test, and the influence of adherend thickness on the measurement of adhesive fracture energy", *Int. J. Adhesion and Adhesives* **18**, 215 (1998).

[2] Price, A. J. and Sargent, J. P., "Small scale aluminium/epoxy peel test specimens and measurement of adhesive fracture energy", *Int. J. Adhesion and Adhesives* **17**(1), 27 (1997).

[3] Moidu, A. K., Sinclair, A. N. and Spelt, J. K., "Analysis of the Peel Test: Prediction of Adherend Plastic Dissipation and Extraction of Fracture Energy in Metal-to-Metal Adhesive Joints", *JTEVA* **23**(4), 241 (1995).
[4] Blackman, B., Dear, J. P., Kinloch, A. J. and Osiyemi, O., "The calculation of adhesive fracture energies from double cantilever beam test specimens", *J. Mat. Sci.* **10**, 253 (1991).
[5] Fernlund, G. and Spelt, J. K., "Mixed mode energy release rates for adhesively bonded beam specimens", *J. Comp. Sci. Tech., and Res.* **16**(3), 234 (1994).
[6] Kaeble, D. H. and Ho, C. L., "Biaxial bond stress analysis in peeling", *Trans. Soc. Rheol.* **18**(2), 219 (1974).
[7] Kim, K.-S. and Aravas, N., "Elastoplastic analysis of the peel test", *Int. J. Solids and Structures* **24**(4), 417 (1988).